frontiers

Supplementary Material: Oxygen Optode Sensors: Principle, Characterization, Calibration and Application in the Ocean.

Henry C. Bittig*, Arne Körtzinger, Craig Neill, Eikbert van Ooijen, Joshua N. Plant, Johannes Hahn, Kenneth S. Johnson, Bo Yang, and Steven R. Emerson

*Correspondence:
Henry Bittig
bittig@obs-vlfr.fr

1 TIME RESPONSE CORRECTION AFTER BITTIG ET AL. (2014)

This is a reproduction of the algorithm shown in Bittig and Körtzinger (2017), Appendix A, based on Bittig et al. (2014). An alternative time response correction algorithm, e.g., used by Fiedler et al. (2013), is described by Miloshevich et al. (2004).

The O_2 optode's time response is governed by the diffusion of O_2 in/out of the sensing foil and trough the liquid boundary layer in front of the sensing foil. In fact, the boundary layer is responsible for most of the "lag". The step response follows (approx.) an exponential curve. The continuous time response equals a single-pole low-pass filter of the in-situ O_2 time series. In discrete form using the bilinear transformation, this filter is recursively described by

$$c^{\mathrm{obs}}(t_{i+1}) = a \cdot c^{\mathrm{obs}}(t_i) + b \cdot \left(c^{\text{in-situ}}(t_{i+1}) + c^{\text{in-situ}}(t_i)\right), \qquad a = 1 - 2\,b, \quad b = \left(1 + 2\,\frac{\tau}{t_{i+1} - t_i}\right)^{-1} \tag{S1}$$

$$c^{\mathrm{obs}}(t_{i=0}) = c^{\text{in-situ}}(t_{i=0}) \tag{S2}$$

where $c^{\text{in-situ}}$ is the true in-situ O_2 time series, c^{obs} the O_2 time series of the optode, and τ the response time for the interval between t_i and t_{i+1}. The initial condition (eq. S2) assumes an equilibrated optode, which can be adjusted according to the application.

For the reconstruction, eq. S1 is rearranged to

$$\frac{c^{\text{in-situ}}(t_{i+1}) + c^{\text{in-situ}}(t_i)}{2} = \frac{1}{2\,b} \cdot \left(c^{\mathrm{obs}}(t_{i+1}) - a \cdot c^{\mathrm{obs}}(t_i)\right), \qquad a = 1 - 2\,b, \quad b = \left(1 + 2\,\frac{\tau}{t_{i+1} - t_i}\right)^{-1} \tag{S3}$$

i.e., knowledge of the optode time series (measurement times, t_i, and optode readings, c^{obs}) as well as the response time (series) τ yields a time series of the consecutive means of the true in-situ time series (left side of eq. S3). For this operation, no initial condition of the filter is required. To obtain the in-situ time

series at the original sampling times t_i, the time series of consecutive means obtained from eq. S3 needs to be interpolated to t_i.

The response time τ can be estimated from a two-layer diffusional model (Bittig et al., 2014) based on an assumption on the sensing membrane thickness l_M and the boundary layer thickness l_L, which is governed by the flow and mode of attachment of the optode. For the SBE63 optode, Bittig et al. (2014) gave an estimate for the silicone PSt3 membrane thickness of $l_M = 130$ μm, of 100 μm for the Aanderaa optodes with standard foil, and of 50 μm for the Aanderaa 4330F optodes with fast response foil. Estimates for l_L for a pumped mode of operation as well as on profiling floats are given in the main manuscript (section 3.4; from Bittig and Körtzinger, 2017). Bittig et al. (2014) give some further indications on the magnitude of l_L for CTD-mounted optodes (range 20 – 50 μm) and the influence of the mode of attachment with respect to the flow direction. The relation between l_L and platform velocity / flow should be refined on a case-by-case basis for such non-standardized platforms.

A graphical representation of the relation between boundary layer thickness l_L, temperature, and response time τ for is given in Bittig et al. (2014) (see also supplementary figure S2), while the numerical values for all three PSt3 membrane thicknesses are provided as supplement to Bittig and Körtzinger (2017).

2 SUPPLEMENTARY FIGURES

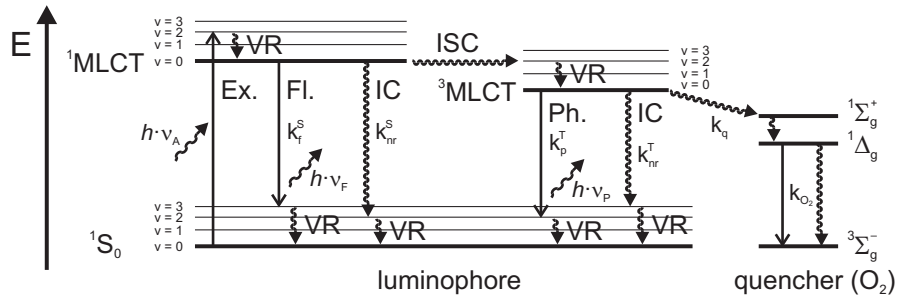

Figure S1: Energy diagram for a luminophore and O_2 as quencher with associated processes: Excitation (Ex.), fluorescence (Fl.), phosphorescence (Ph.), vibrational relaxation (VR), radiationless internal conversion (IC), inter-system crossing (ISC), and collisional quenching by molecular O_2. Molecular term symbols are given for the O_2 triplet ground state ($^3\Sigma_g^-$) and the O_2 singlet excited states ($^1\Sigma_g^+$ with unpaired and $^1\Delta_g$ with paired electrons in the π^* orbit) (after Quaranta et al., 2012).

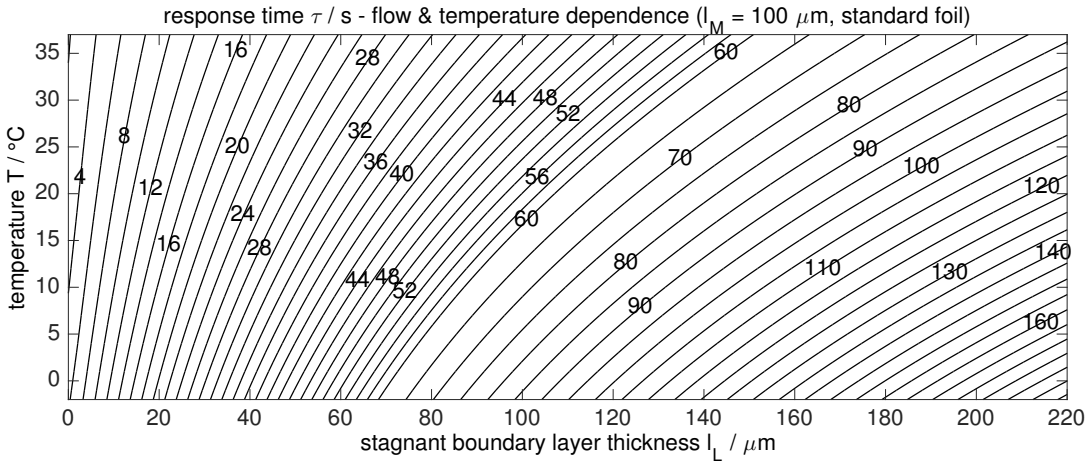

Figure S2: Relation between boundary layer thickness l_L, temperature ϑ, and response time τ for the Aanderaa optode PSt3 standard foil derived after a two-layer diffusional model (Bittig et al., 2014). The numerical data are given in the supplement to Bittig and Körtzinger (2017).

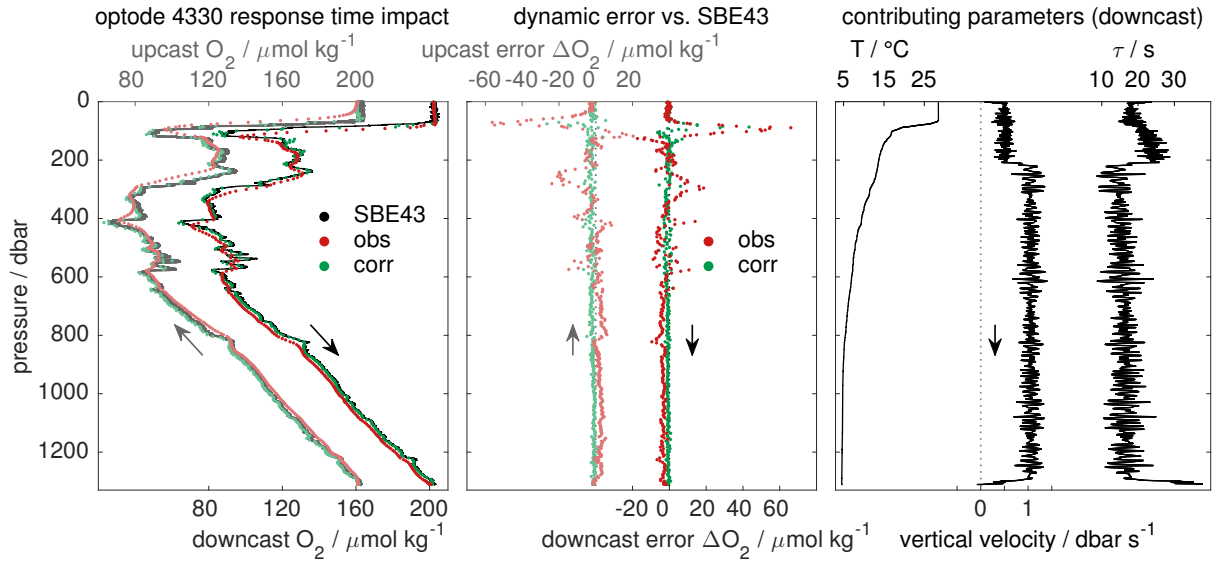

(a)

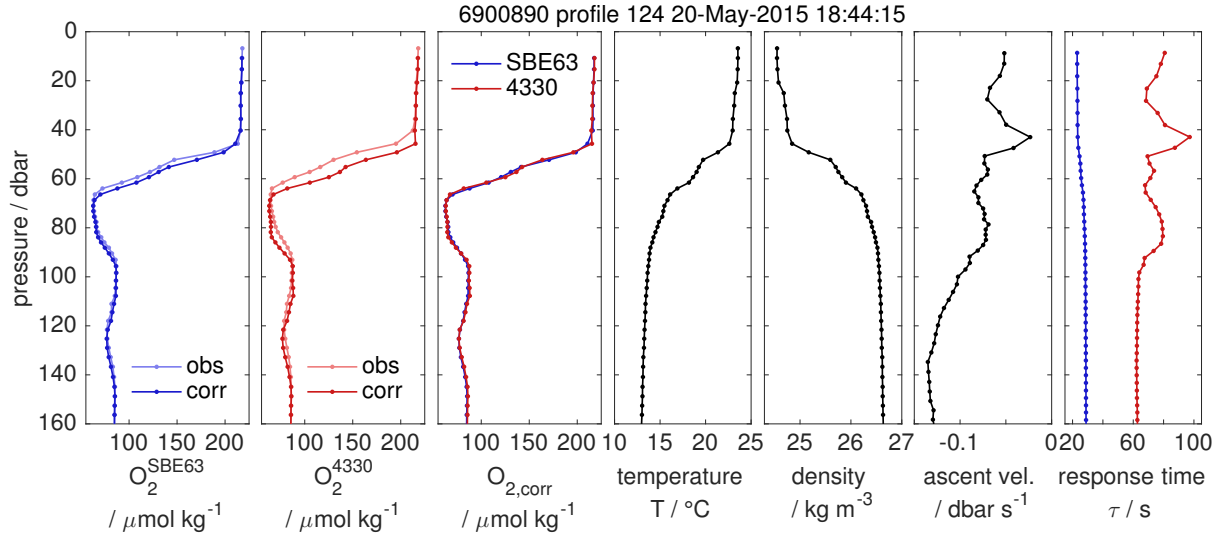

(b)

Figure S3: Example of a dynamic time response correction for (a) a CTD profile with an Aanderaa optode 4330 (after Bittig et al., 2014) and (b) a profile of a dual-O_2 float with both an Aanderaa 4330 (red) and a Sea-Bird SBE63 optode (blue) (after Bittig and Körtzinger, 2017). (a): SBE43 at 24 Hz, optode at 0.2 Hz. The O_2 profile obtained from the SBE43 sensor (black), the 4330 optode (red), and the time response corrected optode data (green) are shown in the left panel. The difference between optode and SBE43 O_2 is given in the middle panel, whereas the right panel gives the environmental conditions (temperature and CTD vertical velocity) that were used to derive an optode response time τ. The left and middle panel show both down- and upcast of the CTD station, whereas the right panel gives only data from the downcast. (b): Panels from left to right give the upper 160 dbar of the Sea-Bird SBE63 optode O_2 observations (pale blue) and time response corrected (deep blue), the Aanderaa 4330 optode O_2 observations (pale red) and time response corrected (deep red), the corrected O_2 data of both Sea-Bird (blue) and Aanderaa optode (red), the temperature profile that to a large extent determines the density profile, which affects the ascent velocity of the buoyancy-driven float, and finally the estimated response time τ for the pumped SBE63 optode (blue) and the unpumped Aanderaa optode (red). The response time of the Aanderaa optode is dependent on the flow and thus the float velocity, in particular for the slow-down in the pycnoline. Apart from the flow, it is modified by temperature, which can be seen both for the pumped SBE63 (i.e., with constant flow) near the surface as well the CTD-attached optode in a.

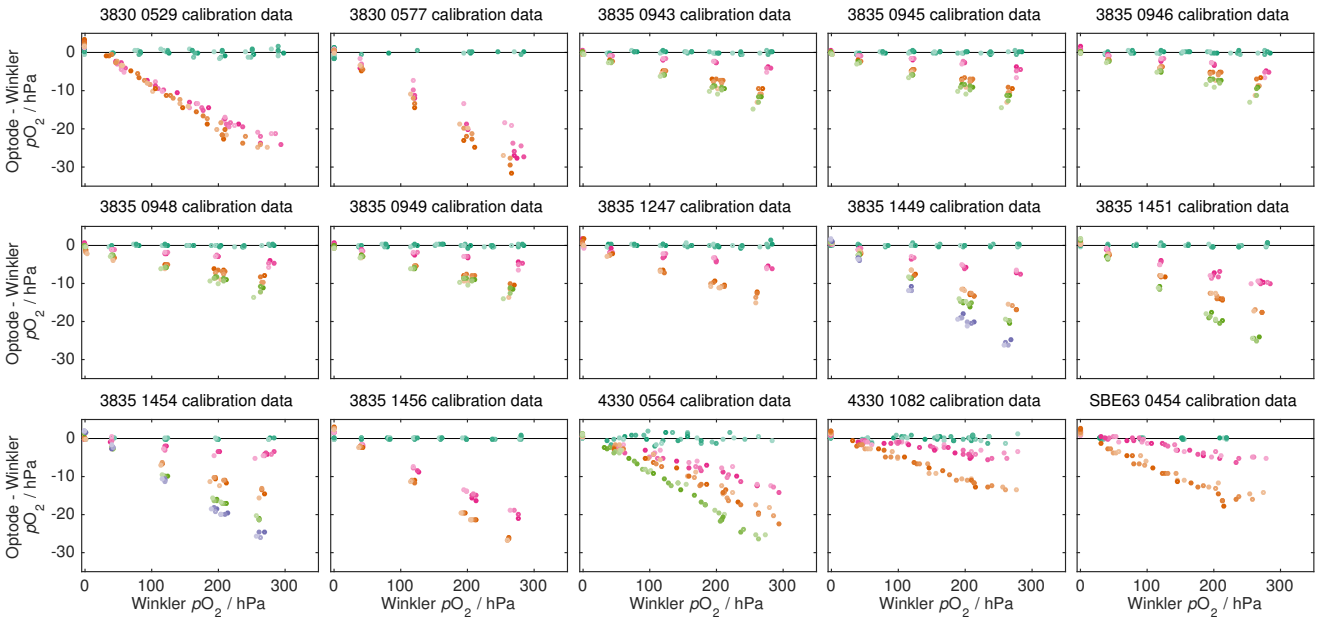

Figure S4: Character of the optode O_2-response drift for 14 Aanderaa optodes and one Sea-Bird optode: Optode drift is linear with oxygen. The difference between optode data and Winkler reference data is plotted against reference pO_2 for a subset of calibrations (colour coded, compare figure 7). Pale colours correspond to data points at cold temperatures. Optode calibration coefficients were derived from the first calibration run.

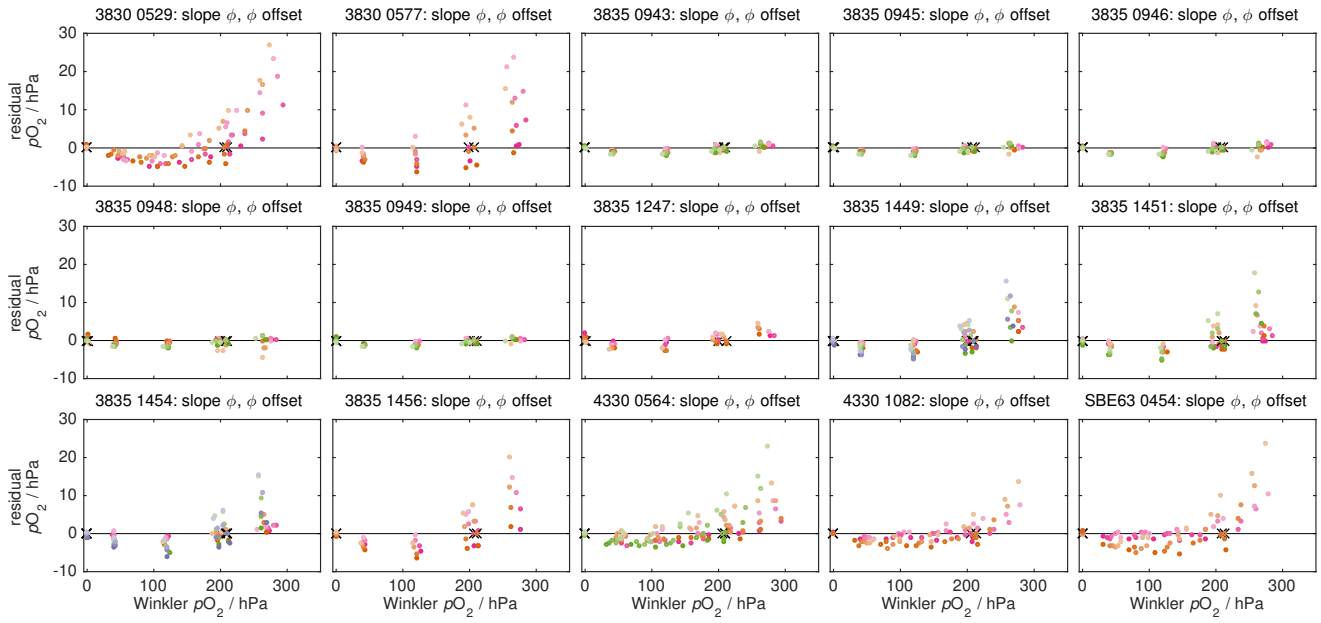

(a)

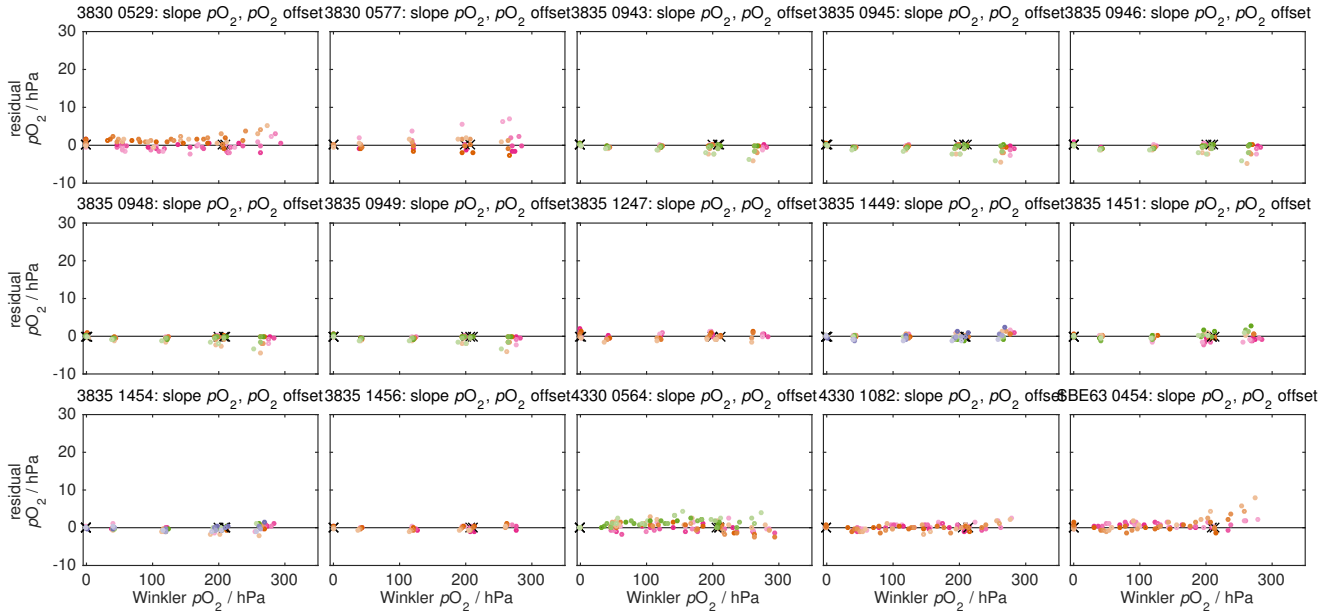

(b)

Figure S5: Comparison of two-point correction approaches of the optode O_2-response drift: Two-point correction (a) with linear phase adjustment (slope and offset on phase) and (b) with linear pO_2 adjustment (slope and offset on pO_2) for 14 Aanderaa optodes and one Sea-Bird optode. The difference between (two-point corrected) optode data and Winkler reference data is plotted against reference pO_2 for a subset of calibrations (colour coded, compare figure 7). Pale colours correspond to data points at cold temperatures. Optode calibration coefficients were derived from the first calibration run. Corrections should be done with a factor on oxygen.

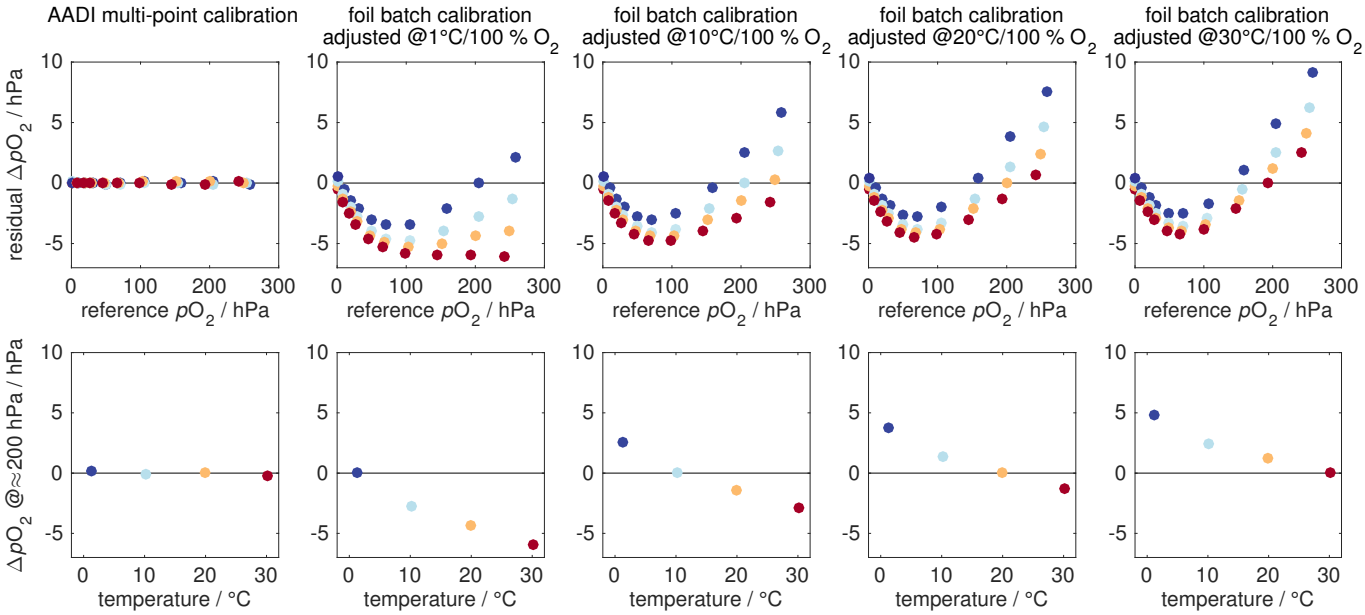

Figure S6: Comparison of Aanderaa multi-point and foil batch calibration for one example (optode 4330 1280, foil ID 1206E). The upper panels show the residual between calibration and multi-point reference data against pO_2, while the lower panels show the temperature dependence of the calibration residuals near 100 % O_2 saturation. The left panels use the multi-point calibration $\mathcal{F}_{\mathrm{multi}}$. The other panels use a foil-batch calibration $\mathcal{F}_{\mathrm{batch}}$ that was two-point adjusted using refit a with one point at 20 °C and 0 % O_2 saturation and one point at 100 % O_2 saturation and 1, 10, 20, or 30 °C, respectively, from the multi-point calibration data. Foil batch-adjusted data show a significant pO_2-temperature residual, i.e., a significant pO_2-temperature slope a (lower panels).

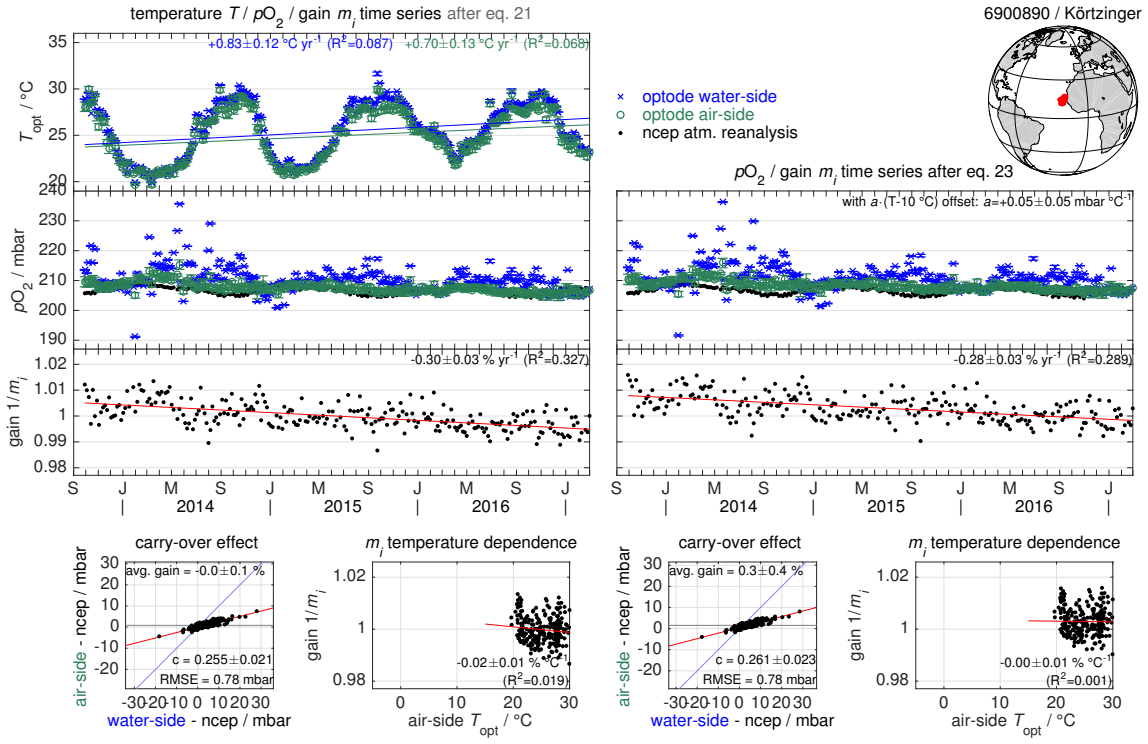

(a)

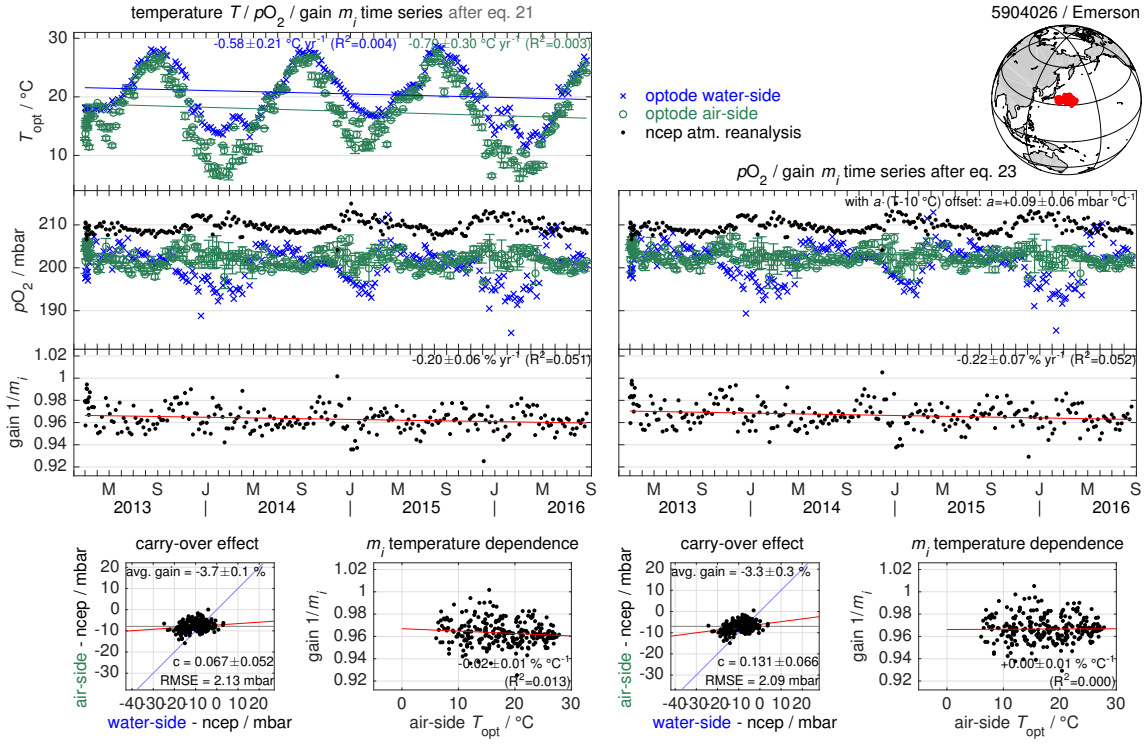

(b)

Figure S7: Optode in-air measurement data for two floats with multi-point laboratory calibration, analyzed after eq. 21 (left) or eq. 23 (right), respectively. Multi-point calibrations provide an adequate O_2-T-response characterization, which is why both a and the $1/m_i$-temperature slopes are close to zero. Both the O_2 correction slope m, its time trend, as well as the carry-over c are insensitive to inclusion of a (eq. 23 vs. eq. 21). Moreover, floats with high optode attachment (Emerson floats, 61 cm stick length) tend to have a near-zero carry-over slope c.

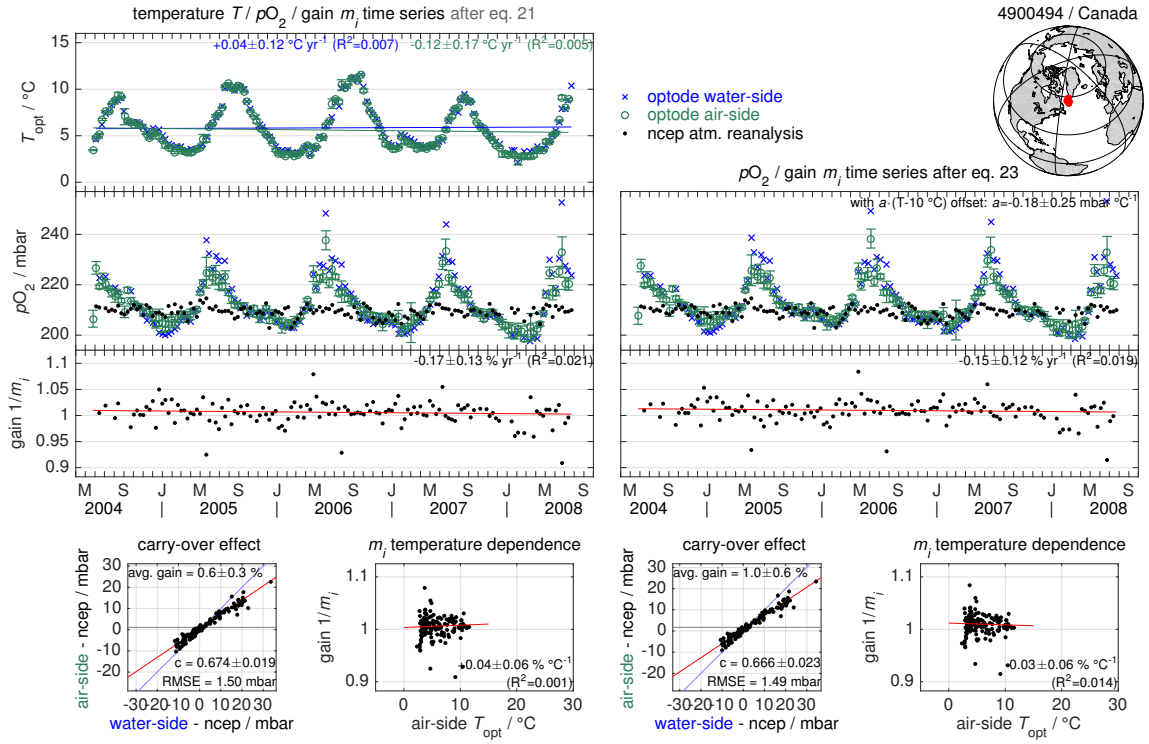
temperature T / pO_2 / gain m_i time series after eq. 21
4900494 / Canada
optode water-side
optode air-side
ncep atm. reanalysis
pO_2 / gain m_i time series after eq. 23
with a·(T-10 °C) offset: a=-0.18±0.25 mbar °C^{-1}
+0.04±0.12 °C yr^{-1} (R^2=0.007)
-0.12±0.17 °C yr^{-1} (R^2=0.005)
-0.17±0.13 % yr^{-1} (R^2=0.021)
-0.15±0.12 % yr^{-1} (R^2=0.019)
T_{opt} / °C
pO_2 / mbar
gain 1/m_i
M S J M S J M S J M S J M S
2004 | 2005 | 2006 | 2007 | 2008
carry-over effect
m_i temperature dependence
avg. gain = 0.6±0.3 %
c = 0.674±0.019
RMSE = 1.50 mbar
0.04±0.06 % °C^{-1}
(R^2=0.001)
air-side - ncep / mbar
water-side - ncep / mbar
air-side T_{opt} / °C
avg. gain = 1.0±0.6 %
c = 0.666±0.023
RMSE = 1.49 mbar
0.03±0.06 % °C^{-1}
(R^2=0.014)

(a)

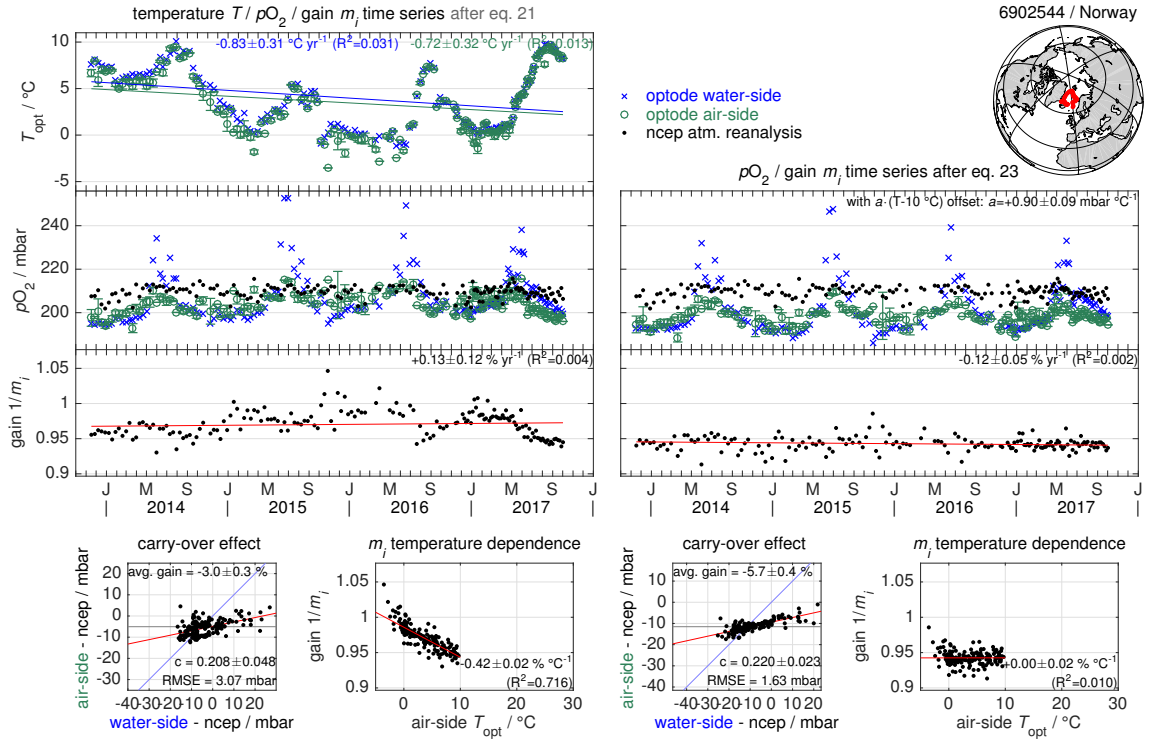
temperature T / pO_2 / gain m_i time series after eq. 21
6902544 / Norway
optode water-side
optode air-side
ncep atm. reanalysis
pO_2 / gain m_i time series after eq. 23
with a·(T-10 °C) offset: a=+0.90±0.09 mbar °C^{-1}
-0.83±0.31 °C yr^{-1} (R^2=0.031)
-0.72±0.32 °C yr^{-1} (R^2=0.013)
+0.13±0.12 % yr^{-1} (R^2=0.004)
-0.12±0.05 % yr^{-1} (R^2=0.002)
T_{opt} / °C
pO_2 / mbar
gain 1/m_i
J M S J M S J M S J M S J
2014 | 2015 | 2016 | 2017 |
carry-over effect
m_i temperature dependence
avg. gain = -3.0±0.3 %
c = 0.208±0.048
RMSE = 3.07 mbar
-0.42±0.02 % °C^{-1}
(R^2=0.716)
air-side - ncep / mbar
water-side - ncep / mbar
air-side T_{opt} / °C
avg. gain = -5.7±0.4 %
c = 0.220±0.023
RMSE = 1.63 mbar
+0.00±0.02 % °C^{-1}
(R^2=0.010)

(b)

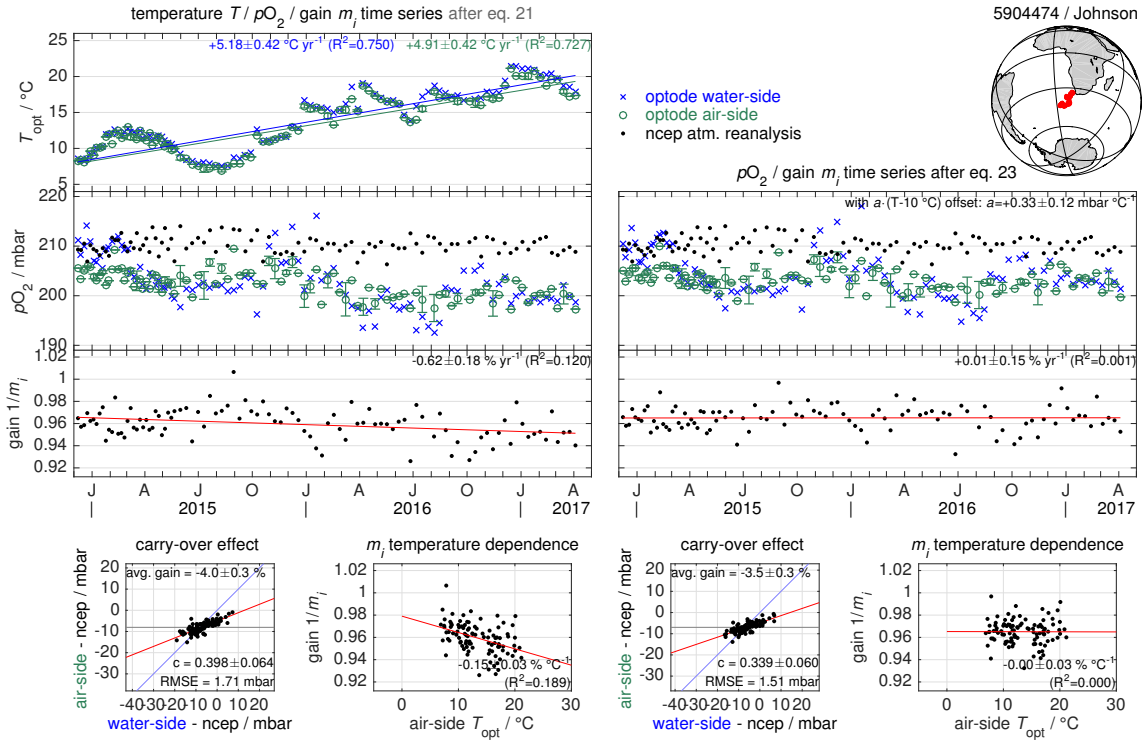

(c)

Figure S8: Optode in-air measurement data for three floats with factory batch calibration, analyzed after eq. 21 (left) or eq. 23 (right), respectively. The pale blue line in the carry-over effect panel gives the 1:1 line, corresponding to air-side optode data being 100 % water pO_2, while the grey horizontal line represents air-side optode data being independent of water pO_2, i.e., 100 % air pO_2. (a) The two-point adjustment for this optode adequately adjusts the foil batch calibration data, i.e., there is no apparent temperature effect on m_i (after eq. 21). Inclusion of the pO_2-T-slope a into the fit gives an insignificant value for a and does not alter any of the other fit parameters. Note the rather strong carry-over effect ($c = 0.67$) for this float. (b) The factory two-point adjustment for this optode is inadequate to represent the O_2-T-response at 100 % O_2 saturation, i.e., there is an apparent temperature effect the further one diverges from 10 °C (left panels, after eq. 21). This is corrected by a, which removes the m_i temperature dependence and thus removes artefacts in the m_i time series, too. The overall fit RMSE is significantly reduced with eq. 23 (see carry-over effect panel) without affecting c or m. (c) The factory two-point adjustment for this optode again is inadequate to represent the O_2-T-response at 100 % O_2 saturation, i.e., there is an apparent temperature effect the further one diverges from 10 °C (left panels, after eq. 21), which is corrected by using eq. 23 (right panels). Together with a strong trend in the temperature time series, such an apparent temperature effect biases the m_i time series, creating apparently large in-situ drift rates (left vs. right m_i time series panels).

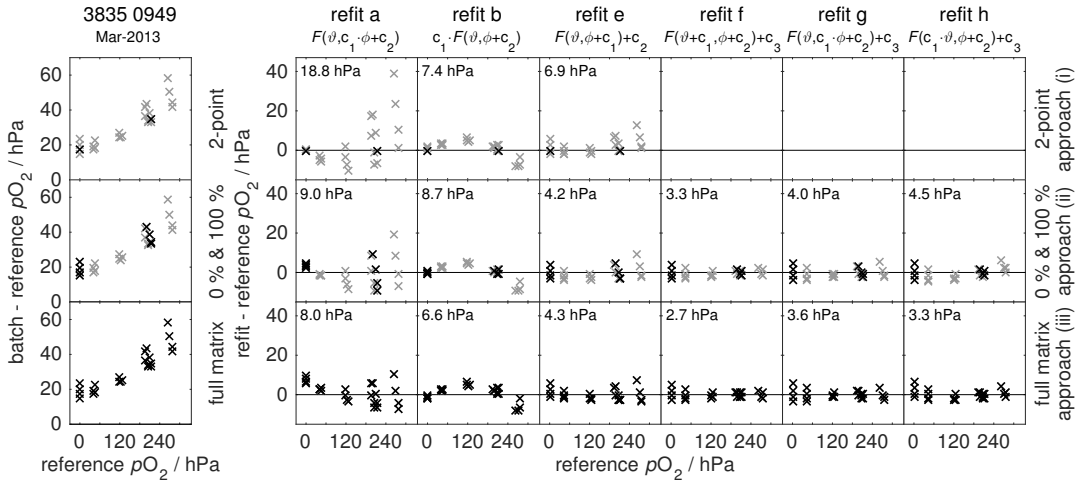

(a)

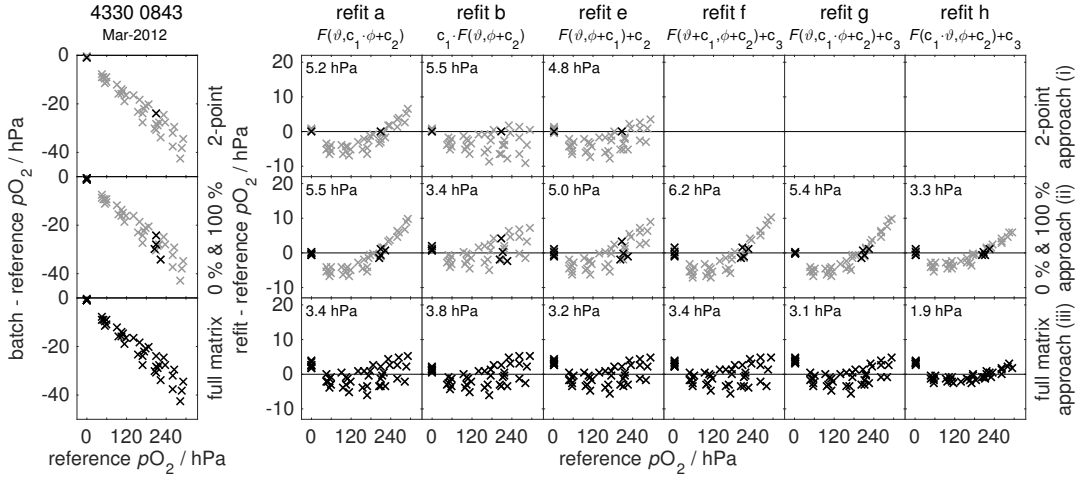

(b)

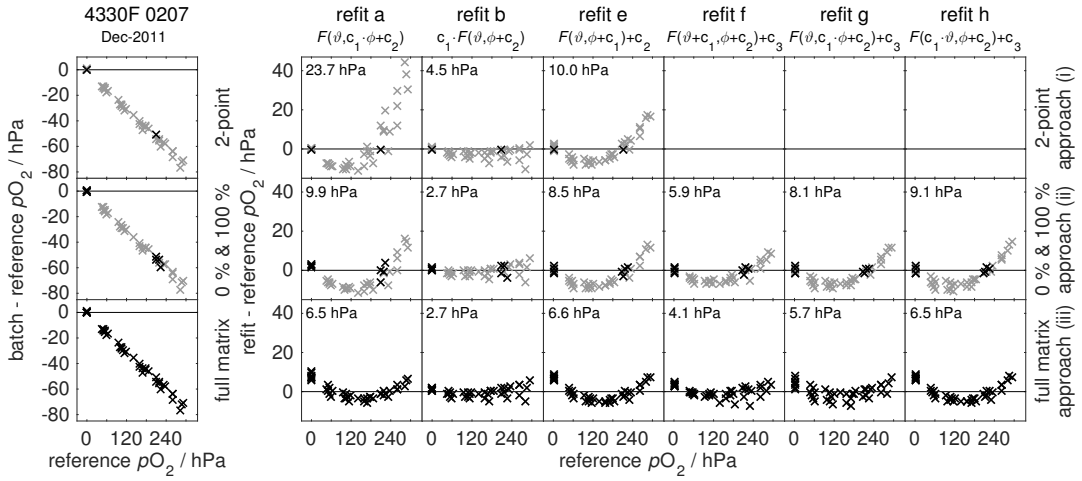

(c)

Figure S9: Batch foil refit examples for an Aanderaa model 3830 (a), 4330 (b), and 4330F (c) optode using the refit equations a, b, and e – h and the three refit approaches i – iii. All multipoint calibration reference data are shown in grey and the subset of points used to constrain the refit parameters c_1, c_2 (and c_3) is denoted in black. The number in the top left corner gives the 90-th percentile of the absolute ΔpO_2 for each refit.

3 SUPPLEMENTARY TABLES

Table S1: Configuration of floats used for the in-air analysis: WMO number; principal investigator (PI) / project name; float type; Aanderaa optode model; optode stick length; average number of samples per cycle and mean interval between samples for near-surface and in-air measurements, respectively; number of cycles with in-air data as well as total number of cycles; local time of the day ($\pm 2\sigma$) if floats surfaced during a particular daytime (otherwise uniform); year and location of the first profile. Körtzinger floats are described in Bittig and Körtzinger (2015), Argo Canada and Johnson floats in Johnson et al. (2015), and Emerson floats in Bushinsky et al. (2016). Floats are ordered by their WMO number. Optodes with individual multipoint laboratory calibration are denoted by diamonds and floats intermittently operating under sea ice by asterisks.

WMO	PI / Project	Float Type	Optode Model	Stick / cm	No. Samples; Δt Surface	No. Samples; Δt Air	No. Cycles Air/Total	Local Daytime	First Profile Year	First Profile Location
4900494	Canada	APEX	3830	10 cm	—	12.7; 14 min	152/153	11±4 h	2004	59.8° N; 049.1° W
4900497	Canada	APEX	3830	10 cm	—	19.2; 37 min	103/104	11±4 h	2004	44.4° N; 055.8° W
4900523	Canada	APEX	3830	10 cm	—	10.4; 33 min	121/125	16±2 h	2004	50.0° N; 148.0° W
4900627	Canada	APEX	3830	10 cm	—	13.4; 43 min	172/175	18±4 h	2005	43.5° N; 057.5° W
4900637	Canada	APEX	3830	10 cm	—	10.8; 24 min	80/165	3±1 h	2005	47.5° N; 130.7° W
4900869	Canada	APEX	3830	10 cm	—	12.8; 18 min	180/181	3±3 h	2006	53.0° N; 145.0° W
4900870	Canada	APEX	3830	10 cm	—	12.8; 17 min	134/135	14±3 h	2006	56.0° N; 141.0° W
4900871	Canada	APEX	3830	10 cm	—	12.4; 32 min	112/161	16±3 h	2006	50.0° N; 145.0° W
4900872	Canada	APEX	3830	10 cm	—	12.7; 19 min	164/165	13±3 h	2006	49.7° N; 138.2° W
4900873	Canada	APEX	3830	10 cm	—	12.5; 34 min	193/195	15±3 h	2006	38.5° N; 145.4° W
4900874	Canada	APEX	3830	10 cm	—	12.6; 44 min	168/169	18±3 h	2006	43.5° N; 138.2° W
4900879	Canada	APEX	3830	10 cm	—	10.5; 27 min	150/151	4±3 h	2006	60.2° N; 048.7° W
4900881	Canada	APEX	3830	10 cm	—	11.8; 44 min	160/163	16±3 h	2006	42.5° N; 061.4° W
4900882	Canada	APEX	3830	10 cm	—	11.9; 34 min	166/168	12±3 h	2006	43.5° N; 057.5° W
4901134	Canada	APEX	3830	10 cm	—	1.2; n/a	89/ 92	7±2 h	2010	48.9° N; 129.2° W
4901135	Canada	APEX	3830	10 cm	—	1.2; n/a	80/ 84	22±2 h	2010	49.5° N; 137.9° W
4901136	Canada	APEX	3830	10 cm	—	1.3; n/a	135/148	0±3 h	2010	50.7° N; 132.0° W
4901137	Canada	APEX	3830	10 cm	—	1.5; n/a	109/123	4±3 h	2010	49.0° N; 131.7° W
4901139	Canada	APEX	3830	10 cm	—	1.3; n/a	129/130	13±3 h	2010	43.8° N; 057.8° W
4901140	Canada	APEX	3830	10 cm	—	1.3; n/a	148/152	0±3 h	2010	44.1° N; 055.9° W
4901142	Canada	APEX	3830	10 cm	—	1.0; n/a	74/ 83	15±3 h	2010	58.2° N; 050.9° W
5903593	Johnson	APEX/UW	3830	10 cm	—	1.5; 27 min	249/268	uniform	2012	65.0° S; 100.7° E
5903612	Johnson	APEX/UW	4330	10 cm	—	1.7; 28 min	216/225	uniform	2011	42.3° S; 008.3° E
5903714	Johnson	APEX/UW	4330	10 cm	—	1.3; 26 min	270/281	uniform	2012	50.0° N; 145.0° W
5903717	Johnson	APEX/UW	3830	10 cm	—	1.5; 28 min	111/298*	uniform	2012	65.0° S; 171.8° E
5903718	Johnson	APEX/UW	3830	10 cm	—	1.4; 25 min	242/250	uniform	2012	49.9° S; 178.1° E
5903743	Emerson	APEX/SOS	4330◇	61 cm	—	35.1; 2 min	288/292	3±7 h	2012	50.0° N; 144.8° W
5903887	Johnson	APEX/UW	3830	10 cm	—	1.5; 27 min	240/294*	uniform	2012	75.4° N; 006.2° W
5904021	Johnson	APEX/UW	4330	10 cm	—	1.4; 25 min	264/267	uniform	2012	35.1° N; 122.9° W
5904025	Emerson	APEX/SOS	4330◇	61 cm	—	28.0; 2 min	272/275	3±3 h	2013	38.2° N; 148.9° E
5904026	Emerson	APEX/SOS	4330◇	61 cm	—	28.0; 2 min	259/265	4±4 h	2013	31.2° N; 146.7° E
5904027	Emerson	APEX/SOS	4330◇	61 cm	—	28.0; 2 min	258/262	4±3 h	2013	33.5° N; 147.6° E
5904028	Emerson	APEX/SOS	4330◇	61 cm	—	28.0; 2 min	265/268	4±3 h	2013	40.5° N; 149.8° E
5904029	Emerson	APEX/SOS	4330◇	61 cm	—	28.9; 2 min	301/301	3±4 h	2013	30.0° N; 146.4° E
5904030	Emerson	APEX/SOS	4330◇	61 cm	—	28.7; 2 min	278/281	3±4 h	2013	32.3° N; 147.1° E

Continued on next page

5904031	Emerson	APEX/SOS	4330◇	61 cm	—	28.8; 2 min	271/275	3±3 h	2013	34.5° N; 148.1° E
5904033	Emerson	APEX/SOS	4330◇	61 cm	—	28.8; 2 min	286/289	3±3 h	2013	39.8° N; 149.7° E
5904104	Johnson	APEX/UW	3830	10 cm	—	1.7; 27 min	171/225*	uniform	2013	63.3° S; 149.2° E
5904105	Johnson	APEX/UW	4330	10 cm	—	1.5; 27 min	89/201*	uniform	2013	65.0° S; 150.1° E
5904124	Johnson	APEX/UW	4330	10 cm	—	1.3; 27 min	220/221	uniform	2013	22.7° N; 157.9° W
5904147	Emerson	APEX/SOS	4330◇	61 cm	—	28.9; 2 min	227/230	3±5 h	2014	15.8° S; 159.0° W
5904179	Johnson	APEX/UW	3830	10 cm	—	1.9; 27 min	108/108	uniform	2014	60.1° S; 174.2° E
5904180	Johnson	APEX/UW	3830	10 cm	—	2.3; 30 min	41/108*	uniform	2014	66.5° S; 156.0° W
5904183	Johnson	APEX/UW	4330	10 cm	—	2.7; 30 min	34/108*	uniform	2014	67.0° S; 150.0° W
5904184	Johnson	APEX/UW	4330	10 cm	—	2.8; 29 min	76/107*	uniform	2014	64.0° S; 150.0° W
5904185	Johnson	APEX/UW	4330	10 cm	—	2.3; 29 min	106/107	uniform	2014	60.0° S; 149.9° W
5904188	Johnson	APEX/UW	4330	10 cm	—	2.4; 28 min	125/144	uniform	2014	49.9° S; 149.9° W
5904395	Johnson	APEX/UW	4330	10 cm	—	1.8; 27 min	142/144	uniform	2014	39.7° S; 150.0° W
5904396	Johnson	APEX/UW	4330	10 cm	—	2.8; 29 min	129/130	uniform	2014	55.0° S; 150.0° W
5904397	Johnson	APEX/UW	4330	10 cm	—	2.7; 31 min	41/ 79*	uniform	2015	61.0° S; 000.0° W
5904467	Johnson	APEX/UW	4330	10 cm	—	1.9; 30 min	45/ 83*	uniform	2014	60.0° S; 000.1° E
5904468	Johnson	APEX/UW	4330	10 cm	—	2.3; 29 min	38/ 79*	uniform	2015	66.0° S; 000.1° E
5904469	Johnson	APEX/UW	4330	10 cm	—	2.3; 28 min	83/ 83	uniform	2014	53.5° S; 000.0° E
5904471	Johnson	APEX/UW	4330	10 cm	—	2.6; 29 min	35/ 82*	uniform	2015	66.9° S; 000.0° W
5904472	Johnson	APEX/UW	4330	10 cm	—	2.6; 30 min	30/ 79*	uniform	2015	67.7° S; 001.8° W
5904474	Johnson	APEX/UW	4330	10 cm	—	1.7; 27 min	98/100	uniform	2014	44.6° S; 007.2° E
5904484	Emerson	APEX/SOS	4330◇	61 cm	—	28.8; 2 min	150/151	3±3 h	2015	17.8° N; 162.1° E
5904485	Emerson	APEX/SOS	4330◇	61 cm	—	28.8; 2 min	152/153	3±3 h	2015	20.2° N; 164.6° E
5904487	Emerson	APEX/SOS	4330◇	61 cm	—	28.8; 2 min	154/154	3±2 h	2014	18.9° N; 163.3° E
6900804	Bulgaria	APEX	3830	10 cm	—	6.1; n/a	165/169	11±2 h	2011	42.7° N; 030.0° E
6900889	Körtzinger	Navis	4330◇	25 cm	5.0; 22 s	10.0; 32 s	175/178	uniform	2014	11.0° N; 023.0° W
6900890	Körtzinger	Navis	4330◇	12 cm	5.0; 22 s	10.0; 32 s	248/259	uniform	2013	16.0° N; 017.6° W
6902544	Norway	APEX	4330	10 cm	—	2.4; n/a	169/174	1±6 h	2013	64.7° N; 000.0° E
6902545	Norway	APEX	4330	10 cm	—	2.3; n/a	136/136	4±2 h	2014	69.3° N; 007.5° E
6902548	Norway	APEX	4330	10 cm	—	1.9; n/a	213/213	23±4 h	2014	68.6° N; 004.7° W
6902549	Norway	APEX	4330	10 cm	—	1.8; n/a	215/215	22±4 h	2014	72.6° N; 001.4° E
6902550	Norway	APEX	4330	10 cm	—	2.0; n/a	213/214	23±4 h	2014	70.8° N; 005.9° E

◇: Optode with individual multipoint laboratory calibration

*: Float intermittently operating under sea ice

Table S2: Results of the in air analysis according to equation 21 (grey; without pO_2-T slope a) and 23 (black; with pO_2-T slope a) for optodes with individual multi-point laboratory calibration. Values in braces give the 95 % confidence interval. Insignificant slopes are shown in italics. Floats are ordered by their mean temperature as in figure 8.

Project / PI	WMO	Optode Model	Length / yr	Temperature Mean $\pm 2\sigma$ / °C	initial pO_2 Slope m_1 at 1st Profile	$1/m_i$ Time Slope / % yr^{-1}	$1/m_i$ Temp. Slope / % °C^{-1}	T Time Slope / °C yr^{-1}	$pO_2 - T$ Slope a / hPa °C^{-1}	Carry-Over Slope c	Fit RMSE / hPa
Emerson	5904147	4330	3.1	+26.6(2.7)	1.025(0.001) 1.025(0.001)	-0.36(0.03) -0.36(0.03)	-0.08(0.03) *-0.01(0.03)*	+0.27(0.08)	– +0.17(0.11)	+0.13(0.12) +0.17(0.10)	1.11 1.14
Emerson	5904484	4330	2.1	+25.9(2.9)	1.025(0.004) 1.025(0.004)	*+0.01(0.09)* *-0.00(0.09)*	*-0.02(0.04)* *+0.01(0.04)*	-0.19(0.12)	– *+0.12(0.18)*	+0.41(0.06) +0.45(0.06)	0.78 0.77
Körtzinger	6900889	4330	2.3	+25.7(2.9)	1.000(0.003) 1.000(0.003)	-0.34(0.05) -0.34(0.04)	+0.06(0.03) *-0.01(0.02)*	+0.12(0.09)	– -0.20(0.12)	+0.25(0.06) +0.18(0.06)	0.77 0.74
Emerson	5904487	4330	2.1	+25.6(3.2)	1.023(0.004) 1.023(0.004)	*-0.01(0.10)* *+0.04(0.13)*	-0.10(0.04) *+0.02(0.05)*	-0.18(0.11)	– +0.44(0.18)	+0.44(0.07) +0.58(0.06)	0.94 0.89
Emerson	5904485	4330	2.1	+25.4(3.8)	1.026(0.004) 1.026(0.004)	+0.19(0.09) +0.25(0.11)	-0.04(0.03) *+0.03(0.04)*	*-0.09(0.12)*	– +0.27(0.15)	+0.40(0.06) +0.52(0.06)	0.98 0.93
Körtzinger	6900890	4330	3.4	+25.1(5.4)	1.000(0.003) 1.000(0.003)	-0.30(0.03) -0.28(0.03)	-0.02(0.01) *-0.00(0.01)*	+0.83(0.12)	– *+0.05(0.05)*	+0.25(0.02) +0.26(0.02)	0.78 0.78
Emerson	5904029	4330	3.9	+23.3(7.6)	1.026(0.001) 1.026(0.001)	-0.18(0.04) *-0.04(0.05)*	-0.09(0.01) *+0.01(0.01)*	+0.96(0.12)	– +0.32(0.08)	*+0.06(0.07)* +0.27(0.05)	2.03 1.76
Emerson	5904031	4330	3.7	+18.6(9.0)	1.041(-0.001) 1.041(-0.001)	-0.31(0.09) *-0.01(0.07)*	-0.28(0.01) *+0.01(0.02)*	+0.30(0.13)	– +0.77(0.09)	*-0.05(0.10)* +0.21(0.05)	3.54 2.14
Emerson	5904026	4330	3.5	+17.5(11.5)	1.038(0.001) 1.038(0.001)	-0.20(0.06) -0.22(0.07)	-0.02(0.01) *+0.00(0.01)*	-0.58(0.21)	– +0.09(0.06)	+0.07(0.05) +0.13(0.05)	2.13 2.09
Emerson	5904025	4330	3.7	+16.9(13.2)	1.065(0.000) 1.065(0.000)	-0.32(0.11) -0.37(0.06)	-0.22(0.01) *+0.00(0.01)*	-0.68(0.29)	– +0.50(0.05)	*+0.02(0.08)* +0.10(0.04)	4.13 2.58
Emerson	5904027	4330	3.5	+16.6(11.0)	1.034(0.000) 1.034(0.000)	*-0.05(0.07)* *-0.05(0.07)*	-0.04(0.01) *-0.00(0.01)*	*+0.15(0.33)*	– +0.07(0.06)	*+0.01(0.03)* *+0.01(0.03)*	2.61 2.60
Emerson	5904033	4330	3.9	+13.2(13.5)	1.036(0.000) 1.036(0.000)	-0.38(0.07) -0.43(0.07)	-0.02(0.01) *+0.00(0.01)*	-1.53(0.26)	– +0.06(0.06)	*+0.02(0.04)* +0.04(0.04)	2.83 2.80
Emerson	5904030	4330	3.7	+11.7(15.2)	1.050(0.000) 1.050(0.000)	-0.11(0.09) -0.20(0.09)	-0.04(0.01) *+0.00(0.01)*	-4.12(0.36)	– +0.08(0.05)	+0.03(0.03) +0.03(0.03)	3.29 3.27
Emerson	5904028	4330	3.6	+10.0(10.9)	1.033(0.001) 1.033(0.001)	-0.17(0.10) *-0.01(0.10)*	-0.09(0.02) *+0.01(0.02)*	+0.82(0.20)	– +0.24(0.09)	+0.12(0.06) +0.20(0.05)	3.05 2.89
Emerson	5903743	4330	4.1	+9.1(6.5)	1.052(0.001) 1.052(0.001)	-0.32(0.02) -0.32(0.02)	*+0.01(0.01)* *-0.00(0.01)*	+0.66(0.10)	– *-0.03(0.05)*	+0.12(0.03) +0.11(0.03)	1.13 1.13

Table S3: Results of the in air analysis according to equation 21 (grey; without pO_2-T slope a) and 23 (black; with pO_2-T slope a) for optodes with factory batch calibration. Values in braces give the 95 % confidence interval. Floats are ordered by their mean temperature as in figure 9.

Project / PI	WMO	Optode Model	Length / yr	Temperature Mean $\pm 2\sigma$ / °C	initial pO_2 Slope m_1 at 1st Profile	$1/m_i$ Time Slope / % yr^{-1}	$1/m_i$ Temp. Slope / % °C^{-1}	T Time Slope / °C yr^{-1}	pO_2-T Slope a / hPa °C^{-1}	Carry-Over Slope c	Fit RMSE / hPa
Johnson	5904124	4330	3.0	+23.8(2.9)	1.068(0.002)	*+0.04(0.06)*	-0.08(0.03)	-0.57(0.07)	–	+0.20(0.11)	1.24
					1.068(0.002)	*-0.08(0.09)*	*+0.03(0.06)*		+0.72(0.33)	+0.54(0.07)	1.20
Canada	4900627	3830	4.8	+21.2(10.4)	0.983(0.007)	+0.26(0.20)	+0.35(0.04)	+1.79(0.39)	–	+0.74(0.05)	1.90
					0.983(0.007)	-0.37(0.13)	*-0.03(0.04)*		-0.78(0.16)	+0.72(0.03)	1.55
Canada	4900497	3830	2.8	+20.1(9.3)	1.008(0.007)	+0.28(0.26)	+0.21(0.05)	+3.23(0.71)	–	+0.73(0.04)	1.59
					1.008(0.007)	-0.19(0.19)	*-0.03(0.03)*		-0.57(0.15)	+0.66(0.03)	1.31
Canada	4901140	3830	4.1	+20.1(11.9)	1.114(0.002)	+0.32(0.07)	+0.02(0.01)	+3.81(0.47)	–	+0.17(0.07)	1.76
					1.114(0.002)	+0.25(0.07)	*-0.00(0.01)*		*-0.05(0.06)*	+0.17(0.06)	1.76
Canada	4901139	3830	3.5	+19.0(13.6)	1.122(0.002)	+0.13(0.13)	-0.03(0.02)	+3.84(0.66)	–	+0.25(0.06)	2.38
					1.122(0.002)	+0.25(0.12)	*+0.00(0.02)*		*+0.07(0.08)*	+0.25(0.06)	2.34
Canada	4900881	3830	4.4	+18.1(14.1)	1.056(0.003)	+0.63(0.13)	+0.21(0.02)	*+0.10(0.75)*	–	+0.35(0.05)	3.12
					1.056(0.003)	+0.57(0.05)	*+0.00(0.01)*		-0.44(0.05)	+0.20(0.04)	1.96
Johnson	5904021	4330	3.8	+16.7(5.0)	1.049(0.002)	+0.03(0.03)	*+0.01(0.01)*	+1.46(0.13)	–	+0.22(0.03)	1.09
					1.049(0.002)	*+0.02(0.03)*	*+0.00(0.01)*		*-0.02(0.06)*	+0.22(0.03)	1.09
Canada	4900882	3830	4.6	+16.3(13.4)	1.059(0.003)	+1.06(0.07)	+0.23(0.01)	+3.26(0.37)	–	+0.25(0.05)	2.97
					1.059(0.003)	+0.32(0.05)	*+0.00(0.01)*		-0.47(0.04)	+0.18(0.03)	1.60
Bulgaria	6900804	3830	2.3	+16.2(13.4)	1.077(0.001)	+0.25(0.25)	-0.25(0.01)	+1.32(0.40)	–	*+0.08(0.09)*	3.78
					1.077(0.001)	+0.21(0.13)	*-0.00(0.01)*		+0.51(0.06)	+0.08(0.04)	2.07
Johnson	5903612	4330	4.3	+16.1(10.0)	1.080(0.003)	-0.24(0.08)	-0.08(0.02)	+3.49(0.23)	–	+0.33(0.05)	2.54
					1.080(0.003)	*+0.01(0.08)*	*+0.00(0.02)*		+0.18(0.08)	+0.31(0.05)	2.46
Canada	4900873	3830	5.3	+15.9(5.9)	1.028(0.006)	+0.26(0.04)	+0.04(0.02)	-0.14(0.11)	–	+0.55(0.05)	0.98
					1.028(0.006)	+0.26(0.04)	*-0.01(0.02)*		-0.11(0.10)	+0.55(0.05)	0.97
Johnson	5904395	4330	3.0	+14.8(4.4)	1.094(0.004)	+0.40(0.09)	-0.18(0.04)	-0.43(0.15)	–	+0.37(0.07)	1.37
					1.094(0.004)	+0.42(0.09)	*-0.01(0.04)*		+0.43(0.19)	+0.42(0.06)	1.25
Johnson	5904474	4330	2.3	+13.4(7.8)	1.042(0.004)	-0.62(0.18)	-0.15(0.03)	+5.18(0.42)	–	+0.40(0.06)	1.71
					1.042(0.004)	*+0.01(0.15)*	*-0.00(0.03)*		+0.33(0.12)	+0.34(0.06)	1.51
Canada	4900874	3830	4.6	+12.6(5.9)	1.054(0.001)	+0.22(0.03)	+0.05(0.02)	+0.16(0.09)	–	+0.13(0.04)	1.11
					1.054(0.001)	+0.22(0.03)	*-0.00(0.02)*		-0.12(0.07)	+0.11(0.04)	1.09
Canada	4900637	3830	4.5	+11.7(6.2)	1.039(0.008)	+0.45(0.25)	*-0.02(0.05)*	+0.31(0.19)	–	+0.76(0.03)	0.90
					1.039(0.008)	+0.43(0.24)	*-0.03(0.05)*		*-0.04(0.24)*	+0.76(0.03)	0.90
Canada	4900879	3830	4.1	+11.6(11.9)	1.058(0.002)	+1.35(0.08)	+0.28(0.01)	+4.46(0.31)	–	+0.22(0.06)	3.17
					1.058(0.002)	+0.17(0.05)	*-0.00(0.01)*		-0.58(0.04)	+0.13(0.02)	1.24
Canada	4901137	3830	3.3	+11.3(6.1)	1.094(0.002)	+0.53(0.09)	*-0.03(0.03)*	+0.31(0.11)	–	+0.20(0.07)	1.63
					1.094(0.002)	+0.52(0.09)	*-0.00(0.03)*		*+0.06(0.14)*	+0.21(0.07)	1.62
Johnson	5903593	3830	3.8	+10.5(3.0)	1.142(0.005)	+0.30(0.15)	-0.63(0.11)	-0.87(0.08)	–	+0.49(0.08)	2.79
					1.142(0.005)	-0.31(0.15)	*+0.00(0.11)*		+1.33(0.50)	+0.50(0.07)	2.58
Canada	4901134	3830	2.5	+10.4(5.5)	1.094(0.001)	+0.52(0.11)	-0.05(0.03)	-0.34(0.24)	–	+0.14(0.05)	1.59
					1.094(0.001)	+0.48(0.11)	*-0.00(0.03)*		*+0.12(0.14)*	+0.16(0.05)	1.55
Johnson	5903714	4330	4.0	+9.9(6.1)	1.105(0.003)	*-0.00(0.03)*	+0.03(0.01)	+0.91(0.10)	–	+0.31(0.02)	0.93
					1.105(0.003)	-0.04(0.03)	*+0.00(0.01)*		-0.08(0.06)	+0.29(0.02)	0.92
Canada	4901135	3830	2.2	+9.0(5.5)	1.082(0.001)	*+0.03(0.14)*	-0.07(0.03)	-0.53(0.19)	–	+0.15(0.07)	1.38
					1.082(0.001)	*-0.03(0.14)*	*+0.00(0.03)*		+0.19(0.16)	+0.19(0.07)	1.34

Continued on next page

Canada	4901136	3830	4.0	+9.0(6.3)	1.083(0.001) 1.083(0.001)	+0.12(0.07) *+0.04(0.07)*	-0.08(0.02) *+0.00(0.02)*	-0.31(0.13)	– +0.17(0.10)	+0.12(0.05) +0.13(0.05)	1.06 0.94
Canada	4900872	3830	4.5	+8.9(6.4)	1.048(0.001) 1.048(0.001)	+0.03(0.03) +0.06(0.03)	+0.03(0.01) *-0.00(0.01)*	-0.67(0.09)	– -0.08(0.05)	+0.12(0.01) +0.10(0.01)	0.95 0.94
Johnson	5904188	4330	3.0	+8.7(2.5)	1.073(0.004) 1.073(0.004)	+0.55(0.11) +0.38(0.11)	-0.40(0.07) *-0.02(0.08)*	-1.09(0.13)	– +0.88(0.32)	+0.38(0.05) +0.41(0.04)	1.56 1.38
Canada	4900871	3830	4.4	+8.4(5.9)	1.046(0.002) 1.046(0.002)	+0.30(0.04) +0.23(0.03)	+0.06(0.02) *-0.00(0.02)*	+0.50(0.09)	– -0.20(0.08)	+0.15(0.03) +0.10(0.03)	1.00 0.92
Canada	4900523	3830	3.4	+8.1(5.8)	1.026(0.006) 1.026(0.006)	*+0.04(0.08)* +0.09(0.07)	+0.08(0.03) *-0.00(0.02)*	-0.83(0.11)	– -0.22(0.11)	+0.56(0.03) +0.53(0.03)	0.97 0.91
Canada	4900869	3830	4.9	+7.9(6.0)	1.042(0.001) 1.042(0.001)	+0.06(0.02) +0.06(0.02)	*+0.01(0.01)* *-0.00(0.01)*	+0.22(0.08)	– *-0.02(0.05)*	+0.14(0.01) +0.14(0.01)	1.14 1.13
Johnson	5904396	4330	2.6	+7.5(3.5)	1.099(0.003) 1.099(0.003)	*+0.04(0.06)* +0.16(0.06)	-0.09(0.02) *-0.00(0.03)*	+1.28(0.16)	– +0.24(0.12)	+0.26(0.03) +0.30(0.03)	0.86 0.80
Norway	6902548	4330	3.2	+7.2(5.2)	1.156(0.002) 1.156(0.002)	-0.27(0.06) -0.18(0.05)	-0.18(0.02) *-0.00(0.02)*	+0.38(0.14)	– +0.42(0.08)	+0.23(0.03) +0.27(0.02)	1.30 1.07
Norway	6902549	4330	3.2	+7.0(5.2)	1.254(0.002) 1.254(0.002)	-0.63(0.06) -0.36(0.05)	-0.24(0.02) *-0.00(0.02)*	+1.13(0.15)	– +0.63(0.09)	+0.18(0.04) +0.25(0.02)	1.58 1.04
Norway	6902545	4330	3.7	+6.8(4.4)	1.065(0.002) 1.065(0.002)	-0.30(0.09) -0.08(0.08)	-0.25(0.04) *-0.00(0.04)*	+0.35(0.12)	– +0.62(0.18)	+0.19(0.04) +0.25(0.03)	1.86 1.59
Canada	4900870	3830	3.7	+6.6(5.8)	1.047(0.001) 1.047(0.001)	-0.25(0.05) -0.19(0.04)	+0.08(0.02) *+0.00(0.02)*	-0.45(0.09)	– -0.22(0.08)	+0.14(0.02) +0.12(0.02)	1.08 0.98
Canada	4900494	3830	4.2	+5.7(4.8)	0.994(0.007) 0.994(0.007)	-0.17(0.13) -0.15(0.12)	*+0.04(0.06)* *-0.03(0.06)*	*+0.04(0.12)*	– *-0.18(0.25)*	+0.67(0.02) +0.67(0.02)	1.50 1.49
Norway	6902550	4330	3.2	+5.5(5.9)	1.155(0.002) 1.155(0.002)	*-0.06(0.07)* -0.26(0.06)	-0.17(0.02) *+0.00(0.02)*	-2.03(0.19)	– +0.35(0.08)	+0.19(0.02) +0.20(0.02)	2.23 1.80
Johnson	5904179	3830	3.0	+5.0(2.9)	1.126(0.002) 1.126(0.002)	+0.27(0.07) +0.37(0.06)	-0.18(0.04) *-0.00(0.04)*	+0.45(0.08)	– +0.40(0.20)	+0.16(0.06) +0.19(0.05)	1.42 1.36
Johnson	5903718	3830	3.5	+4.9(7.2)	1.168(0.003) 1.168(0.003)	-0.42(0.06) *-0.05(0.05)*	+0.12(0.02) *-0.00(0.02)*	-3.18(0.15)	– -0.25(0.06)	+0.27(0.04) +0.22(0.04)	1.55 1.39
Canada	4901142	3830	2.2	+3.8(6.8)	1.062(0.002) 1.062(0.002)	*-0.01(0.30)* *+0.23(0.28)*	+0.10(0.06) *+0.00(0.05)*	-2.19(0.58)	– *-0.23(0.24)*	+0.21(0.06) +0.19(0.06)	2.60 2.50
Norway	6902544	4330	3.9	+3.5(6.8)	1.030(0.002) 1.030(0.002)	+0.13(0.12) -0.12(0.05)	-0.42(0.02) *+0.00(0.02)*	-0.83(0.31)	– +0.90(0.09)	+0.21(0.05) +0.22(0.02)	3.07 1.63
Johnson	5903887	3830	4.2	+2.6(5.8)	1.156(0.002) 1.156(0.002)	+0.43(0.04) +0.29(0.04)	+0.12(0.02) *-0.00(0.02)*	+1.01(0.13)	– -0.36(0.09)	+0.24(0.02) +0.18(0.02)	2.20 1.87
Johnson	5904185	4330	3.0	+1.7(2.9)	1.083(0.002) 1.083(0.002)	-0.10(0.09) +0.23(0.06)	-0.33(0.04) *-0.00(0.04)*	+0.89(0.15)	– +0.73(0.18)	+0.23(0.06) +0.26(0.04)	1.46 1.17
Johnson	5904104	3830	4.1	+0.5(3.0)	1.114(0.005) 1.114(0.005)	+0.45(0.20) +0.40(0.17)	+0.30(0.15) *+0.03(0.13)*	+0.79(0.09)	– -0.90(0.65)	+0.49(0.04) +0.41(0.05)	3.79 3.60
Johnson	5904469	4330	2.3	+0.2(2.0)	0.996(0.003) 0.996(0.003)	*+0.14(0.22)* +0.17(0.16)	-0.90(0.11) *-0.00(0.11)*	+0.13(0.10)	– +1.95(0.52)	+0.25(0.09) +0.30(0.06)	2.10 1.53
Johnson	5904397	4330	2.2	+0.1(2.6)	1.189(0.002) 1.189(0.002)	-0.87(0.15) -0.21(0.15)	-0.62(0.09) *+0.02(0.09)*	+0.71(0.24)	– +1.84(0.55)	+0.22(0.12) +0.37(0.05)	1.66 1.00
Johnson	5904468	4330	2.2	+0.1(2.6)	1.026(0.002) 1.026(0.002)	-0.73(0.22) *-0.06(0.15)*	-0.72(0.10) *+0.01(0.08)*	+0.58(0.17)	– +1.93(0.46)	+0.23(0.07) +0.29(0.03)	2.27 1.48
Johnson	5904471	4330	2.3	+0.0(2.2)	1.022(0.002) 1.022(0.002)	-0.62(0.18) -0.25(0.18)	-0.46(0.12) *-0.02(0.13)*	+0.76(0.16)	– +1.22(0.65)	+0.19(0.09) +0.27(0.06)	1.45 1.12
Johnson	5904467	4330	2.3	-0.1(2.5)	1.162(0.001) 1.162(0.001)	*+0.01(0.12)* *+0.04(0.12)*	*-0.03(0.08)* *+0.00(0.08)*	+0.41(0.20)	– *+0.09(0.37)*	+0.11(0.06) +0.11(0.06)	1.23 1.23

Continued on next page

Johnson	5904184	4330	3.0	-0.2(3.2)	1.056(0.002) 1.056(0.002)	*+0.08(0.15)* +0.47(0.11)	-0.45(0.06) *-0.01(0.06)*	+0.86(0.13)	– +1.05(0.28)	+0.17(0.08) +0.24(0.06)	3.03 2.26
Johnson	5904180	3830	3.0	-0.4(1.7)	1.105(0.004) 1.105(0.004)	+0.80(0.27) +0.20(0.11)	+0.88(0.26) *+0.05(0.12)*	+0.78(0.10)	– -2.27(0.54)	+0.45(0.11) +0.15(0.08)	1.70 1.38
Johnson	5904472	4330	2.2	-0.5(1.9)	1.003(0.001) 1.003(0.001)	-0.71(0.22) -0.59(0.14)	-0.50(0.19) *+0.01(0.18)*	+0.43(0.22)	– +1.93(0.93)	+0.10(0.08) +0.21(0.05)	2.01 1.70
Johnson	5904105	4330	3.6	-0.6(3.5)	1.031(0.003) 1.031(0.003)	-0.47(0.21) *+0.03(0.20)*	-0.88(0.10) *+0.01(0.12)*	+0.96(0.17)	– +2.14(0.45)	+0.25(0.13) +0.36(0.08)	4.39 2.50
Johnson	5903717	3830	5.1	-1.0(1.7)	1.112(0.001) 1.112(0.001)	+0.10(0.08) +0.17(0.06)	+0.71(0.13) *+0.06(0.12)*	-0.08(0.05)	– -1.80(0.59)	+0.13(0.05) *+0.04(0.04)*	3.25 3.05
Johnson	5904183	4330	3.0	-1.1(1.3)	1.139(0.001) 1.139(0.001)	+0.50(0.10) +0.49(0.10)	*-0.01(0.19)* *-0.01(0.19)*	*-0.04(0.11)*	– *-0.11(0.82)*	+0.14(0.09) +0.13(0.09)	1.21 1.21

Table S4: Example of O_2 quantity conversions using the SCOR WG 142 recommendations (Bittig et al., 2016) for 100 % O_2 saturation, a pO_2 partial pressure of 205 hPa, and an O_2 concentration of 250 μmol L^{-1}, both in freshwater and at a salinity of 35, at the sea surface and at 2000 dbar (set quantities denoted by asterisks). The ranges in the converted quantities mainly depend on temperature due to the temperature dependence of solubility (O_2 saturation $\leftrightarrow$ O_2 concentration and O_2 partial pressure $\leftrightarrow$ O_2 concentration conversions). Atmospheric pressure has a small impact on the O_2 saturation $\leftrightarrow$ O_2 concentration as well as for the O_2 saturation $\leftrightarrow$ O_2 partial pressure conversion.

Salinity	P / dbar	O_2 sat. / %	pO_2 / hPa	O_2 conc. / μmol L^{-1}	O_2 conc. / μmol kg^{-1}
0	0	100*	195 – 215	225 – 460	225 – 460
35	0	100*	195 – 215	190 – 360	185 – 350
0	2000	100*	195 – 215	175 – 345	175 – 345
35	2000	100*	195 – 215	145 – 270	140 – 260
0	0	95 – 105	205*	230 – 445	230 – 445
35	0	95 – 105	205*	195 – 350	190 – 340
0	2000	95 – 105	205*	180 – 335	180 – 335
35	2000	95 – 105	205*	150 – 265	145 – 255
0	0	55 – 110	115 – 220	250*	≈250
35	0	70 – 130	150 – 265	250*	≈244
0	2000	75 – 140	155 – 285	250*	≈250
35	2000	95 – 170	195 – 340	250*	≈244

REFERENCES

Bittig, H. C., Fiedler, B., Scholz, R., Krahmann, G., and Körtzinger, A. (2014). Time response of oxygen optodes on profiling platforms and its dependence on flow speed and temperature. *Limnol. Oceanogr.: Methods* 12, 617–636. doi:10.4319/lom.2014.12.617

Bittig, H. C. and Körtzinger, A. (2015). Tackling oxygen optode drift: Near-surface and in-air oxygen optode measurements on a float provide an accurate in situ reference. *J. Atmos. Oceanic Technol.* 32, 1536–1543. doi:10.1175/JTECH-D-14-00162.1

Bittig, H. C. and Körtzinger, A. (2017). Technical note: Update on response times, in-air measurements, and in situ drift for oxygen optodes on profiling platforms. *Ocean Sci.* 13, 1–11. doi:10.5194/os-13-1-2017

Bittig, H. C., Körtzinger, A., Johnson, K. S., Claustre, H., Emerson, S., Fennel, K., et al. (2016). SCOR WG 142: Quality Control Procedures for Oxygen and Other Biogeochemical Sensors on Floats and Gliders. Recommendations on the conversion between oxygen quantities for Bio-Argo floats and other autonomous sensor platforms. doi:10.13155/45915

Bushinsky, S. M., Emerson, S. R., Riser, S. C., and Swift, D. D. (2016). Accurate oxygen measurements on modified Argo floats using in situ air calibrations. *Limnol. Oceanogr.: Methods* 14, 491–505. doi:10.1002/lom3.10107

Fiedler, B., Fietzek, P., Vieira, N., Silva, P., Bittig, H. C., and Körtzinger, A. (2013). In situ CO_2 and O_2 measurements on a profiling float. *J. Atmos. Oceanic Technol.* 30, 112–126. doi:10.1175/JTECH-D-12-00043.1

Johnson, K. S., Plant, J. N., Riser, S. C., and Gilbert, D. (2015). Air Oxygen Calibration of Oxygen Optodes on a Profiling Float Array. *J. Atmos. Oceanic Technol.* 32, 2160–2172. doi:10.1175/JTECH-D-15-0101.1

Miloshevich, L. M., Paukkunen, A., Vömel, H., and Oltmans, S. J. (2004). Development and Validation of a Time-Lag Correction for Vaisala Radiosonde Humidity Measurements. *J. Atmos. Oceanic Technol.* 21, 1305–1327. doi:10.1175/1520-0426(2004)021⟨1305:DAVOAT⟩2.0.CO;2

Quaranta, M., Borisov, S. M., and Klimant, I. (2012). Indicators for optical oxygen sensors. *Bioanal. Rev.* 4, 115–157. doi:10.1007/s12566-012-0032-y